

# THE SKY DISTRIBUTION OF 511 KEV POSITRON ANNIHILATION LINE EMISSION AS MEASURED WITH INTEGRAL/SPI

G. Weidenspointner<sup>1</sup>, J. Knödlseher<sup>1</sup>, P. Jean<sup>1</sup>, G.K. Skinner<sup>1</sup>, P. von Ballmoos<sup>1</sup>, J.-P. Roques<sup>1</sup>, G. Vedrenne<sup>1</sup>, P. Milne<sup>2</sup>, B.J. Teegarden<sup>3</sup>, R. Diehl<sup>4</sup>, A. Strong<sup>4</sup>, S. Schanne<sup>5</sup>, B. Cordier<sup>5</sup>, and Ch. Winkler<sup>6</sup>

<sup>1</sup>Centre d'Etude Spatiale des Rayonnements, BP 4346, 31028 Toulouse Cedex 4, France

<sup>2</sup>Steward Observatory, 933 N. Cherry Ave., Tucson, AZ, 85721, USA

<sup>3</sup>NASA/GSFC, LHEA, Greenbelt, MD 20771, USA

<sup>4</sup>Max-Planck-Institut für extraterrestrische Physik, 85740 Garching, Germany

<sup>5</sup>DSM/DAPNIA/SAP, CEA Saclay, Gif-sur-Yvette, France

<sup>6</sup>ESA/ESTEC, SCI-SD, 2201 AZ Noordwijk, The Netherlands

## ABSTRACT

The imaging spectrometer SPI on board ESA's INTEGRAL observatory provides us with an unprecedented view of positron annihilation in our Galaxy. The first sky maps in the 511 keV annihilation line and in the positronium continuum from SPI showed a puzzling concentration of annihilation radiation in the Galactic bulge region. By now, more than twice as many INTEGRAL observations are available, offering new clues to the origin of Galactic positrons. We present the current status of our analyses of this augmented data set. We now detect significant emission from outside the Galactic bulge region. The 511 keV line is clearly detected from the Galactic disk; in addition, there is a tantalizing hint at possible halo-like emission. The available data do not yet permit to discern whether the emission around the bulge region originates from a halo-like component or from a disk component that is very extended in latitude.

Key words: Galactic 511 keV line emission; positron annihilation.

## 1. INTRODUCTION

The detection of 511 keV positron annihilation line emission from the central region of our Galaxy was one of the early and important successes of gamma-ray astronomy [17, 22]. Although positron annihilation gives rise to the strongest gamma-ray line signal from our Galaxy, three decades of dedicated observational and theoretical effort have fallen short of unveiling the origin of Galactic positrons. A large variety of potential astrophysical and exotic positron sources have been proposed, including: interactions of cosmic rays in the interstellar medium [32]; pulsars [39] and millisecond pulsars [44]; the decay of radioactive nuclei expelled by supernovae [6], novae [7], Wolf-Rayet stars [29], or hypernovae/gamma-

ray bursts [3]; compact objects harbouring black holes or neutron stars [33], low-mass X-ray binaries [30], and micro-quasars [12]; gamma-ray bursts [23]; pair production by gamma rays from so-called Small Mass Black Holes with X-ray photons from the supermassive black hole at the center of our Galaxy, Sgr A\* [41]; interactions of cosmic rays accelerated during episodes of mass accretion onto the supermassive black hole Sgr A\* [5, 42]; and decay or annihilation of (light) dark matter [35, 2] or other exotic particles and processes [see e.g. references in 1].

Investigations of the sky distribution of the annihilation radiation promise to provide clues for the identification of the source(s) of positrons in our Galaxy. Positrons may travel from their birth places before annihilating, however, recent theoretical work suggests that positron diffusion is limited [15, 10]. Thus the Galactic distribution of annihilation radiation can be expected to resemble that of the positron sources.

First maps of the annihilation radiation, limited to the inner regions of our Galaxy, were obtained using the OSSE instrument on board the Compton Gamma-Ray Observatory in the 511 keV line and in positronium continuum emission [e.g. 31, 4, 24, 25, 26, 27]. Some of these analyses also took advantage of data obtained with the Gamma-Ray Spectrometer on board the Solar Maximum Mission (SMM) and the TGRS spectrometer on board the Wind satellite. Furthermore, the OSSE instrument allowed Kinzer, Purcell, & Kurfess [18] and Kinzer et al. [19] to study the one-dimensional distribution in longitude and in latitude of diffuse emission, including annihilation radiation, from the inner Galaxy.

With the commissioning of the imaging spectrometer SPI on board ESA's INTEGRAL observatory, high spectral resolution mapping with improved angular resolution has become feasible [13, 46, 20, 38, 47]. Both the 511 keV line emission and the positronium continuum emission were found to be brightest in a region of a few degrees around the Galactic center; emission from the Galac-

tic disk is much fainter, implying that positron annihilation is concentrated in the central regions of our Galaxy [20, 38, 47]. In particular, the high bulge-to-disk flux ratio of 1–3 (corresponding to a luminosity ratio of 3–9) measured in the annihilation line imposes severe constraints on potential positron sources. The most promising positron sources for the Galactic bulge were found to be members of the old stellar population, specifically Type Ia supernovae (SN Ia) and/or low-mass X-ray binaries (LMXBs). Annihilation or decay of light dark matter was another possibility. At least part of the faint emission from the Galactic disk must be due to the  $\beta^+$ -decay of the radioisotopes  $^{26}\text{Al}$  and  $^{44}\text{Ti}$  which are produced by massive members of the young stellar population. However, none of these positron sources is without caveats [see e.g. 20, 12, 36].

Additional insight into the origin, propagation, and annihilation of positrons can be obtained from high-resolution spectroscopy. The detailed shape of the annihilation line and the ratio of the fluxes in the line and the positronium continuum depend on the physical conditions of the interstellar medium in which positrons annihilate [see e.g. 11]. Using observations of the Galactic bulge, Jean et al. [15] showed that positrons annihilate in the warm phase of the interstellar medium. Recently, Beacom & Yüksel [1] pointed out that spectroscopy of Galactic emission above 511 keV can be used to set an upper limit on the initial energy at which positrons are injected into the interstellar medium [see also 37].

In this contribution, we present the current status of our studies of the large-scale distribution of Galactic 511 keV annihilation line radiation using more than 2 years of observations with the spectrometer SPI. An update on SPI spectroscopy of positron annihilation radiation is given in a companion paper by Jean et al. [16]. After describing our analysis methods, we first present an updated sky map in the 511 keV line. We then summarize our current results regarding the distribution of the bright 511 keV line emission from the Galactic center region and regarding the existence and distribution of more extended emission from the Galactic disk and beyond.

## 2. INSTRUMENT AND DATA ANALYSIS

The SPI imaging spectrometer consists of an array of 19 actively cooled high resolution Ge detectors, which cover an energy range of 20–8000 keV with an energy resolution of about 2.1 keV FWHM at 511 keV. SPI employs an active anti-coincidence shield made of bismuth germanate (BGO), which also acts as a collimator. In addition to its spectroscopic capabilities, SPI can image the sky with moderate spatial resolution of about  $3^\circ$  FWHM using a tungsten coded aperture mask. The fully coded field-of-view of the instrument is about  $16^\circ$ . A detailed description of the instrument was given by Vedrenne et al. [43].

The results presented here are based on a data set that

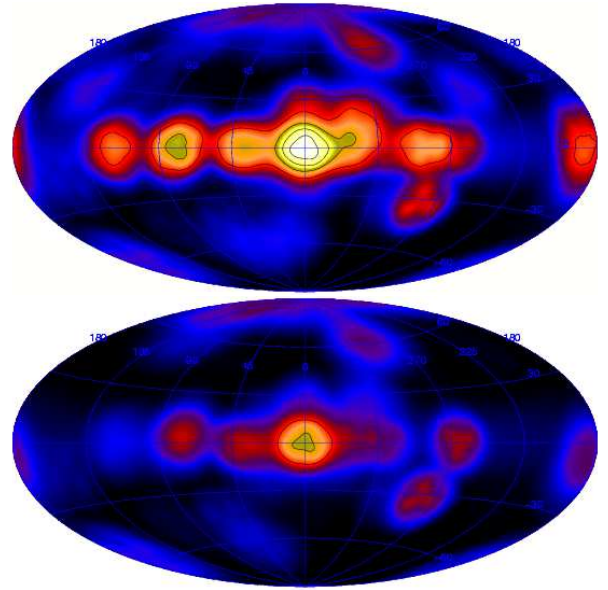


Figure 1. Top panel: the exposure to the sky of the data set used in this analysis. Contour levels are at 1, 2, 3, and  $4 \times 10^7 \text{ cm}^2 \text{ s}$ . Bottom panel: the exposure to the sky after the first year of the mission, depicted with the same color coding than above. Contour levels are at 1 and  $2 \times 10^7 \text{ cm}^2 \text{ s}$ .

comprises more than twice as many observations as that we used in our studies after the first year of the mission [20, 15, 47]. Specifically, we have used the April 20, 2006 public INTEGRAL data release (i.e. three-day orbital revolutions 16-269, 277, 278, 283-285). These public data were supplemented by instrument team observations of the Galactic center region and of the Galactic plane and by recent private observations of SNR 1006, Cen X-4, and Sco X-1 up to revolution 423. The observations were taken during the epoch November 23, 2002 through April 1, 2006. During this time a few very strong (notably during October 2003 and September 2005), and several smaller, solar flares occurred. These resulted in strong transient enhancements of the instrumental background at 511 keV. These exceptional periods were removed, resulting in a cleaned data set that consists of 18101 pointings with a combined live time of  $3.6 \times 10^7 \text{ s}$ .

The resulting exposure to the sky is depicted in the top panel of Fig. 1; for comparison, the exposure from the observations of the first year of the mission is shown in the bottom panel. To a first approximation, the exposure of the current data set is about twice that achieved after the first year. Of particular importance for the analyses presented here is the fact that the exposure along the Galactic plane not only deepened, but also became more homogeneous within about  $|l| < 90^\circ$ . However, unfortunately the substantial inhomogeneity outside that region has not been alleviated. The exposure is still deepest around the central region of our Galaxy, and most of the remaining, lower, exposure away from that region is still concentrated in a rather narrow band of  $\pm 10^\circ$  along the inner part of the Galactic disk. Investigations of the large-

scale distribution of 511 keV line annihilation therefore still face the dilemma that regions of putative faint and extended emission remain poorly exposed. Specifically, the current inhomogeneity of exposure severely limits our ability to distinguish between models for low surface brightness emission outside the bulge region. This is particularly pertinent to investigating a potential halo distribution around the Galactic bulge, and to determining the latitude distribution of the disk emission.

In our analyses, we followed the procedures for modelling the instrumental background that we established earlier [for more details, see e.g. 20]. The count rate in the detectors is the sum of time variable instrumental background and signal from celestial sources. The latter is variable in time because even if the celestial source is intrinsically stable SPI's exposure to it varies in time as the instrument performs a series of observations. Source components have therefore to be distinguished from the dominant background components by taking advantage of their differing time variations. Hence our approach for extracting the source components consists of fitting time series of detector count rates by a linear combination of so-called background templates (time series of background components, explained below) and mask modulated signals.

We performed our analyses in a 5 keV wide energy interval centered at 511 keV<sup>1</sup>. In this energy range the instrumental background consists of two components: the instrumental 511 keV background line, and an underlying continuum background [14, 45, 40]. The variations in time of these two background components differ, so they are modelled independently [20]. The time variation of the 511 keV background line is modelled using a linear combination of three templates, the rate of saturating ( $> 8$  MeV) events in the Ge detectors (GeDsats), a constant, and a linear increase in time. In this context, a template represents a specific time series of background count rates in a given detector. The role of the first two templates is to account for prompt and short-lived background components, the third template accounts for long-lived background components. The time variation of the continuum background underlying the instrumental 511 keV line is modelled by assuming it is identical (per unit energy) to that observed in an adjacent energy interval, for which we chose 523–545 keV. To reduce statistical uncertainties, the continuum time variation was smoothed [see 20].

When applying this 4-component background model, the normalizations of the three line background components are adjusted independently for each detector to account for detector-to-detector variations of the instrumental background. In addition, the normalizations of the

<sup>1</sup>When varying the width of the analysis energy interval, the bulge flux varies as expected from the spectral results by Jean et al. [15]. Based on their two-Gaussian model for the 511 keV line spectrum, the flux determined in our 5 keV analysis interval corresponds to 82% of the total line flux. The variation of the disk flux is consistent with that of the bulge flux; detailed spectroscopy results from the current data set are reported in Jean et al. [16].

GeDsats component are adjusted for each orbital revolution, as in model ORBIT-DETE described in Knödlseeder et al. [20]. An additional complication arises from the fact that during the epoch covered by our data set, two SPI detectors failed (detector 2 on Dec. 7, 2003, or IJD 1435, and detector 17 on Jul. 17, 2004, or IJD 1659). Each time a detector fails, the detector-to-detector ratio of the instrumental background changes significantly, especially in the 511 keV background line and for detectors next to the failed detector. We therefore split the data set into three periods, each corresponding to a stable detector configuration, and simultaneously apply three separate ORBIT-DETE models.

### 3. RESULTS

#### 3.1. Imaging

To obtain a model independent sky map of the 511 keV positron annihilation line radiation, we employed the Multi-Resolution Expectation Maximization (MREM) algorithm described in Knödlseeder et al. [21]. This algorithm is an extension of the implementation of the Richardson-Lucy (RL) algorithm that we applied in earlier analyses [e.g. 20].

The resulting sky map is depicted in Fig. 2. As in earlier SPI analyses of the positron annihilation line [20] and the positronium continuum [47], the only prominent 511 keV line signal is that seen from the central region of our Galaxy. Any emission from other sky regions is much fainter. We are investigating the effect of the noise filtering threshold on MREM maps, as well as the effect of smoothing scales on RL maps, in an effort to determine the best approach for uncovering faint and extended annihilation emission that we detect by model fitting (see Sec. 3.2).

As with the first year observations, we find again that the centroid of the emission is close to the Galactic center. The dominant emission from the central Galaxy appears to be more concentrated than seen in the first year observations. This conclusion is confirmed by model fitting (see Sec. 3.2). The total flux in the map is about  $1.0 \times 10^{-3}$  ph cm<sup>-2</sup> s<sup>-1</sup>.

#### 3.2. Model Fitting

A more quantitative approach for studying the Galactic distribution of the observed extended line emission is model fitting, which we performed using a maximum likelihood multi-component fitting algorithm described in Knödlseeder et al. [20]. In the present work, our focus is on investigating whether there is 511 keV line emission outside the central region of the Galaxy. In particular, we are trying to characterize the emission from the Galactic disk, and to assess whether there is evidence for emission

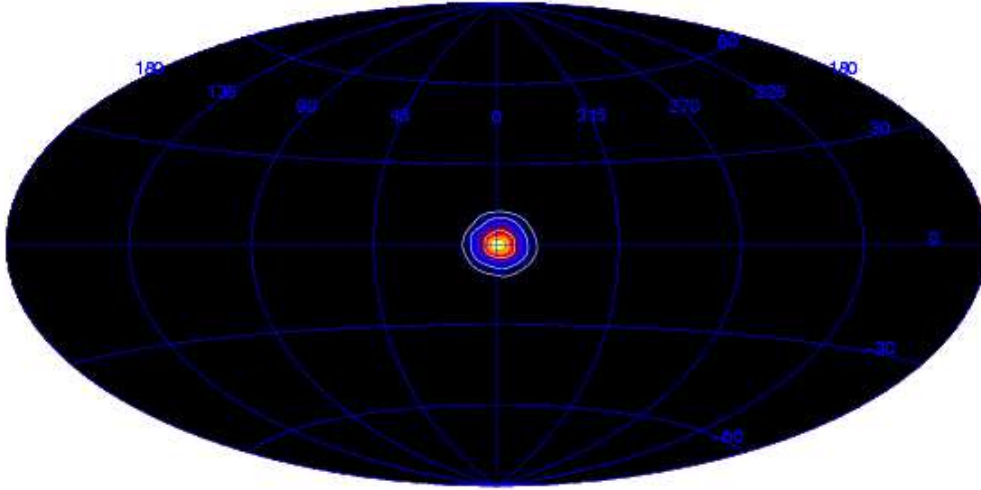


Figure 2. An MREM sky map of the 511 keV positron annihilation line emission. The contours indicate intensity levels of  $10^{-2}$ ,  $10^{-3}$ , and  $10^{-4}$   $\text{ph cm}^{-2} \text{s}^{-1} \text{sr}^{-1}$ . Details are given in the text.

from a halo component. In the first year data, disk emission was already marginally detected, while a stellar halo component (comprising emission peaking at the Galactic center and fainter emission extending far beyond the bulge region) could not yet be discerned from pure bulge models.

In order to investigate the possible existence of faint and extended emission from outside the central region of the Galaxy we fitted simple and flexible models for bulge and halo emissions in the absence or presence of simple disk models. The bulge and halos emissions were represented by nested spherical shells of homogeneous emissivity, centered at the Galactic center. The disk emission was described either by the young (0–0.15 Gyr) or the old (7–10 Gyr) stellar disk models as derived by Robin et al. [34]. The fit results are summarized in Table 1.

It is evident from Table 1 that there is significant 511 keV line emission from outside the bulge region of the Galaxy. The maximum likelihood ratio  $\lambda$  for the “2 nested shells” bulge model is only 1273.8, much lower than for any other model tested. Adding a halo component (i.e. shells extending farther from the Galactic center) and/or a disk model significantly improves the fits. The disk models are favoured over the halo models since either disk model improves the fit more than additional shell/halo components. In any combination of halo and disk components, the disk component is always significantly detected. When combined with a disk, the 1.5–5 kpc shell is still marginally detected, which provides a tantalizing hint at possible halo-like emission; the 5–8 kpc shell is then not required. The fluxes from the two innermost shells, describing the bulge region, are remarkably robust and independent of the presence of other model components, reflecting the brightness of the bulge region of our Galaxy in annihilation radiation. For the two-shell “bulge only” model, we obtain a total flux of  $(0.96 \pm 0.06) \times 10^{-3} \text{ph cm}^{-2} \text{s}^{-1}$ , in excellent agreement with Knödlseeder et al. [20]. For all other mod-

els in Table 1, we obtain total fluxes in the range  $(1.7\text{--}3.1) \times 10^{-3} \text{ph cm}^{-2} \text{s}^{-1}$ . Considering only models including disk components, but excluding models with four shells (since the large flux attributed to the 5–8 kpc shell is very uncertain), we obtain bulge+halo fluxes in the range  $(0.8\text{--}1.3) \times 10^{-3} \text{ph cm}^{-2} \text{s}^{-1}$  and disk fluxes in the range  $(0.9\text{--}1.8) \times 10^{-3} \text{ph cm}^{-2} \text{s}^{-1}$ . The bulge-to-disk (B/D) flux ratio is found to be between 0.4 and 1.4. These values are lower than the range 1–3 determined by Knödlseeder et al. [20] using the first year of SPI observations. Although mostly consistent within statistical errors, we tend to find now lower bulge fluxes and higher disk fluxes than with the first year data. Our values for the B/D flux ratio lie within the wide range of 0.2–3.3 obtained by Milne et al. [24] from OSSE/SMM/TGRS observations.

We then investigated other characterizations of the bulge and disk emission. In a first step, and to compare with previous work, we modelled the bulge emission using an ellipsoidal distribution with a Gaussian radial profile in longitude and latitude, with full-widths at half maximum in longitude and latitude  $\Gamma_l$  and  $\Gamma_b$ . This bulge model was combined with the young stellar disk description by Robin et al. [34]; its three parameters are the disk scale length  $h_{R+}$ , the scale length of the central disk hole  $h_{R-}$ , and the axis ratio  $\epsilon$  [see definitions in Table 3 of [34]]. We find values of  $\Gamma_l = 6.5^{+1.1}_{-0.9}^\circ$  and  $\Gamma_b = 5.1^{+0.8}_{-0.8}^\circ$  for the bulge component. These values indicate a bulge extent that is slightly smaller than the FWHM of about  $8^\circ$  inferred from the first year data [20]. We note that Kinzer et al. [19] found values of  $\Gamma_l = 6.3^\circ \pm 1.5^\circ$  and  $\Gamma_b = 4.9^\circ \pm 0.7^\circ$  in an analysis of OSSE observations, in very good agreement with our measurement. The parameter values for the disk component are  $h_{R+} \sim 4$  kpc,  $h_{R-} \sim 3$  kpc, and  $\epsilon \sim 0.3$ . As will be discussed below, none of these disk parameters is well constrained by the current data (for comparison, the young stellar disk is defined by  $h_{R+} = 5$  kpc,  $h_{R-} = 3$  kpc, and  $\epsilon = 0.014$ ). Our disk parameters correspond to

Bulge/Halo Model	Bulge/Halo Flux [ph cm <sup>-2</sup> s <sup>-1</sup> ]	Old Stellar Disk Flux [ph cm <sup>-2</sup> s <sup>-1</sup> ]	$\lambda$
Dwek et al. (1995) stellar bulge E3	$(8.67 \pm 0.38) \times 10^{-4}$	$(1.62 \pm 0.29) \times 10^{-3}$	1281.1
Dwek et al. (1995) stellar bulge G3	$(8.48 \pm 0.36) \times 10^{-4}$	$(1.60 \pm 0.29) \times 10^{-3}$	1295.4
Freudenreich (1998) stellar bulge S	$(8.87 \pm 0.39) \times 10^{-4}$	$(1.57 \pm 0.30) \times 10^{-3}$	1262.7
Freudenreich (1998) stellar bulge E	$(8.87 \pm 0.39) \times 10^{-4}$	$(1.56 \pm 0.30) \times 10^{-3}$	1264.1
Robin et al. (2003) stellar halo	$(2.35 \pm 0.10) \times 10^{-3}$	$(1.16 \pm 0.30) \times 10^{-3}$	1319.6

Table 2. The results of fits to the 511 keV line data of the preferred triaxial or bar-shaped stellar bulge models E3 and G3 by Dwek et al. [8] and S and E by Freudenreich [9], and of the stellar halo model by Robin et al. [34].  $\lambda$  is the maximum likelihood ratio of the fits.

a FWHM in longitude of about  $70^\circ$  for the 511 keV line emission, which is about twice as large as found by Kinzer et al. [19] with OSSE. The maximum likelihood ratio for this model is  $\lambda = 1315.4$ , and the bulge and disk fluxes are  $(7.04 \pm 0.32) \times 10^{-4}$  ph cm<sup>-2</sup> s<sup>-1</sup> and  $(1.41 \pm 0.17) \times 10^{-3}$  ph cm<sup>-2</sup> s<sup>-1</sup>, respectively. In this case, the B/D flux ratio is about 0.5. Considering the number of model parameters that have been optimized, this description of the data using an ellipsoidal bulge and a very extended (in latitude) disk is not statistically superior to the two-shell bulge models combined with a stellar disk (compare Table 1).

Rather than changing the aspect ratio of the Gaussian, more improvement is possible by changing the profile. The bulge model can be improved by using e.g. two Gaussian distributions instead of one ellipsoidal distribution. The values for the FWHM of the two Gaussians are  $2.1^{+1.4}_{-1.5}^\circ$  and  $8.0^{+2.3}_{-1.0}^\circ$ , respectively. The value of  $\lambda$  rises to about 1325, indicating that the 511 keV emission may be peaked or cusped at the Galactic center. The fluxes in the narrow and wide Gaussian and in the disk model are about  $1.5 \times 10^{-4}$  ph cm<sup>-2</sup> s<sup>-1</sup>,  $7.4 \times 10^{-4}$  ph cm<sup>-2</sup> s<sup>-1</sup>, and  $1.3 \times 10^{-3}$  ph cm<sup>-2</sup> s<sup>-1</sup>, respectively. Now the B/D flux ratio is about 0.7.

To further investigate the distribution of the dominant annihilation radiation from the central region of the Galaxy, we also fitted to the 511 keV data some astrophysical models, namely the preferred triaxial or bar-shaped stellar bulge models E3 and G3 by Dwek et al. [8] and S and E by Freudenreich [9], and the stellar halo model by Robin et al. [34], each combined with the old stellar disk. The results are summarized in Table 2. The stellar bar models E3, G3, S, and E provide rather poor descriptions of the emission from the bulge region, compared to the simple shell models summarized in Table 1, and compared to ellipsoidal or Gaussian descriptions. It therefore appears that the distribution of the 511 keV line emission does not follow the stellar bulge. The stellar halo model of Robin et al. [34], however, provides a fit that is of similar quality than that of the best analytical models. As will be discussed below (see Sec. 4), it is too early to conclude that indeed halo emission around the Galactic center region exists. The good agreement between data and stellar halo model may mainly be due to the fact that it models well the peaked emission at the Galactic center. The ex-

istence of a sharp peak in the emission is already hinted at by the good fit provided by the two-Gaussian bulge model described above. For the stellar halo model (which includes bulge emission), the total 511 keV line flux is about  $2.35 \times 10^{-4}$  ph cm<sup>-2</sup> s<sup>-1</sup>, and the (bulge+halo)-to-disk flux ratio is about 2. This is consistent with the earlier analysis of Knödlseher et al. [20] and also with estimates of halo fluxes by OSSE/SMM/TGRS [24, 28].

Our final step to date in investigating whether there is 511 keV line emission outside the central region of the Galaxy, and whether it can be uniquely described by rather simple models, was to vary the axis ratio parameter in the Robin et al. [34] young and old disk models. Combined with either the two-shell (see Table 1), with an ellipsoidal ( $\Gamma_l = 6.5^\circ$  and  $\Gamma_b = 6.0^\circ$ ) description of the bulge emission, or with the stellar halo model by Robin et al. [34]. As an example, for the young disk the variation of the maximum likelihood ratio  $\lambda$  with the axis ratio  $\epsilon$  for the three descriptions of the emission from the central region of the Galaxy are depicted in Fig. 3. The results for the old stellar disk are similar. We note that the axis ratios for the Robin et al. [34] young (0–0.15 Gyr) and old (7–10 Gyr) stellar disks are 0.014 and 0.0791, respectively. For both bulge models, the preferred axis ratio is about 0.3, much larger than the young disk value, in particular. The uncertainty is, however, rather large. For the stellar halo, the preferred value of  $\epsilon$  is similar to those for the Robin et al. [34] stellar disks, and the uncertainty is much smaller. These results clearly demonstrate that there is faint, extended emission around the central region of the Galaxy, but with the current data it is impossible to decide whether this emission is due to a halo-like component, or a disk very extended in latitude.

As mentioned above, we have begun to study the longitude distribution of the Galactic 511 keV line emission by determining the best-fit values not only for the axis ratio  $\epsilon$ , but also for the disk scale length  $h_{R+}$  and for the scale length of the central hole  $h_{R-}$  for the Robin et al. [34] young stellar disk parameterization. Their best fit parameters correspond to a FWHM in longitude of about  $70^\circ$  for the 511 keV line emission. We have also begun to study the longitude distribution by dividing the disk emission into longitude bins. First results indicate that we do not yet detect 511 keV emission from disk regions that are more than  $50^\circ$  in longitude from the Galactic center.

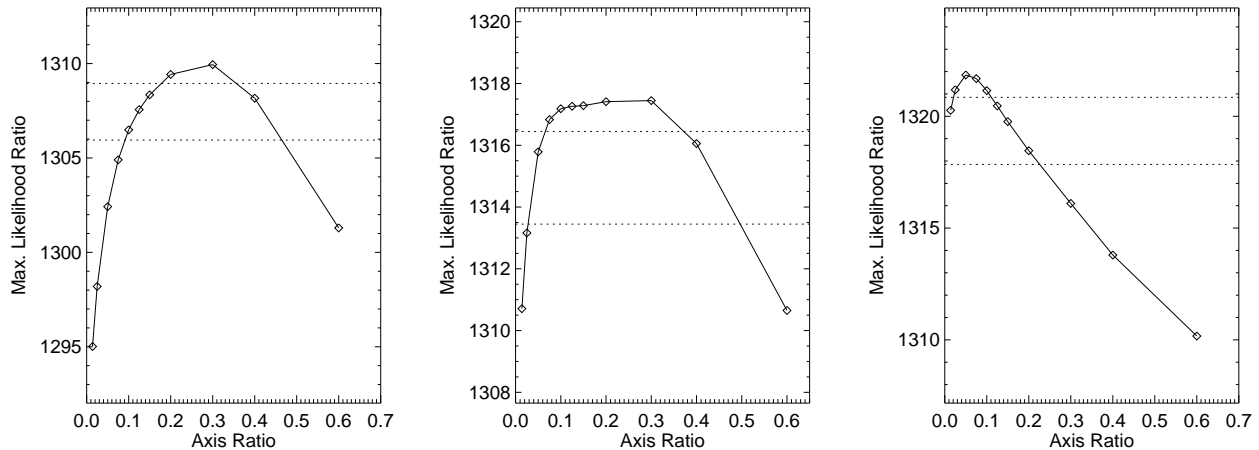


Figure 3. Left panel: the variation of the maximum likelihood ratio  $\lambda$  when fitting the data with the Robin et al. [34] young disk plus an ellipsoidal model (FWHM  $\Gamma_l = 6.5^\circ$  and  $\Gamma_b = 6.0^\circ$ ) of the bulge emission. Center panel: as left panel, except that the bulge emission is modelled by a combination of 0–0.5 kpc and 0.5–1.5 kpc homogeneous shells. Right panel: as left and center panels, except that the emission from the central region of the Galaxy is described by the stellar halo model of Robin et al. [34]. The dashed lines indicate decreases of  $\lambda$  by 1 and 4, corresponding to 1 and  $2\sigma$  confidence levels for 1 degree of freedom.

Both results indicate that 511 keV line emission is brightest from the inner Galaxy. More exposure, in particular in the outer Galaxy, will be required to better determine the longitude profile.

#### 4. SUMMARY AND DISCUSSION

The analyses we have performed to date, taking advantage of more than 2 years of observations, clearly demonstrate that SPI detects 511 keV annihilation line emission from outside the central or bulge region of the Galaxy. In similar, earlier analyses using only the first year of observations, the disk was only marginally detected by SPI, while the emission from the central region of the Galaxy could statistically be equally well described by pure bulge or bulge and halo distributions. Before the launch of INTEGRAL, positron annihilation from the Galactic disk had already been detected using OSSE observations, sometimes supplemented by SMM and TGRS data [e.g. 24, 19]. However, constraining the spatial characteristics of the disk emission, in particular its latitude distribution, eluded OSSE/SMM/TGRS, as did a conclusive result regarding the existence of halo emission.

While SPI has not yet solved these two major goals of positron astronomy, the current status of our studies with SPI does represent significant progress and promises much more. SPI now detects disk emission at a significance level of about  $6\sigma$  (see e.g. Table 1), thus confirming the earlier detections with the OSSE/SMM/TGRS instruments. In addition, with SPI we find tantalizing hints at possible halo-like emission. When representing the halo-like emission by extended shells as in Table 1, we detect the 1.5–5 kpc shell at the  $\sim 2.5\sigma$  level even when a disk model is included in the fit. Another indication for po-

tential halo emission is the good fit of the emission from the central region of the Galaxy provided by the stellar halo model of Robin et al. [34], which comprises emission peaking at the Galactic center and fainter emission extending far beyond the bulge region. Finally, the existence of faint, extended emission around the Galactic bulge region is demonstrated by the fact that when a halo component is not included in the model disks with very wide latitude extents are favoured. When describing the central emission with a stellar halo, the preferred latitude extent of the disk is much smaller (see Fig. 3).

Despite this tantalizing indications for halo-like emission, some caution is in order because of the inhomogeneous exposure to the sky (see Fig. 1). With the current exposure to the sky, we cannot exclude that most or all of the flux attributed to the 1.5–5 kpc shell model is actually originating from the Galactic disk, particularly in case the disk is extended in latitude. Similarly, the stellar halo model by Robin et al. [34] may describe the emission from the central region of the Galaxy well mainly because the model is rather peaked or cusped at the Galactic center. The existence of such a peak or cusp is indicated by the good fit provided by the two-Gaussian (FWHM about  $2.1^\circ$  and  $8.0^\circ$ ) bulge model. Since both the emission and the exposure are maximal around the Galactic center, it is possible that the fits result is driven by a rather small sky area in the bulge. Lower surface brightness emission around the bulge would fall in sky regions that have received relatively little exposure. They therefore carry comparatively little weight in the fitting.

More observations around the Galactic bulge region will be needed to alleviate the existing systematic biases due to the current inhomogeneity of the exposure. With the existing data, we cannot yet discern whether the emission around the bulge region originates from a halo-like com-



ponent or from a disk component that is very extended in latitude. In particular, the latitude distribution of the disk cannot be determined independently of assumptions about the distribution of emission in and around the bulge region. Thus the situation reached with the INTEGRAL data with more than 2 years of data already starts to improve on what was possible with the combination of data from OSSE/SMM/TGRS at the end of the 9 year CGRO mission [24, 28]. It is hoped that INTEGRAL will continue to operate for many years and make further advances possible.

The current data indicate that the disk is brightest in 511 keV line emission in the inner Galaxy. Preliminary results indicate a FWHM in longitude of about  $70^\circ$  for the 511 keV line emission, which is about twice as large as determined by Kinzer et al. [19] with OSSE. More exposure, in particular in the outer Galaxy, will be required to better determine the longitude profile.

Using the first year of SPI observations, the emission from the central region of the Galaxy could be equally well described by various astrophysical stellar bulge and halo distributions, or simple analytical shapes [20]. With the current, increased data set this is no longer true. The preferred stellar bulge models derived by Dwek et al. [8] and Freudenreich [9] from COBE observations in the infra-red provide a poorer fit of the 511 keV line distribution than simple analytical functions. It therefore appears that the distribution of the 511 keV line emission does not follow the stellar bulge. Of all astrophysical distributions that we tested, only the stellar halo model by Robin et al. [34] could compete. However, given the lack of an independent detection of genuine halo emission from outside the bulge region and the inhomogeneity of the exposure, it is possible that the halo model fares well mainly because it provides a good description of the brightest emission close to the Galactic center. The good quality of the halo model fit, and the results from attempts at fitting the bulge emission with more than a single ellipsoid, indicate that within a few degrees from the Galactic center the annihilation emission exhibits some sort of “peak” or “cusp”. More observations will be needed to further investigate whether the emerging sub-structure of annihilation radiation from the complex bulge region can be associated with gas and/or source distributions. The flux attributed to the stellar halo is consistent with the earlier analysis of Knödlseeder et al. [20] and also with estimates of halo fluxes by OSSE/SMM/TGRS [24, 28].

The analyses reported here are ongoing; more refined results will be presented elsewhere, including searches for point sources. Looking at the years ahead, reducing the inhomogeneity of the exposure of the central region of the Galaxy is crucial for studying the large-scale distribution of annihilation radiation. More observations around the Galactic bulge region in particular, but also above and below the disk, will be needed to alleviate the currently existing systematic uncertainties.

## ACKNOWLEDGEMENTS

Based on observations with INTEGRAL, an ESA project with instruments and science data centre funded by ESA member states (especially the PI countries: Denmark, France, Germany, Italy, Switzerland, Spain), Czech Republic and Poland, and with the participation of Russia and the USA.

## REFERENCES

- [1] Beacom, J.F., & Yüksel, H., 2006, *Phys. Rev. Lett.*, 97, 071102
- [2] Boehm, C., et al., 2004, *Phys. Rev. Letters*, 92, 1301
- [3] Cassé, M., et al., 2004, *ApJ*, 602, 17
- [4] Chen, L.X., et al., 1997, *ApJ*, 481, L43
- [5] Cheng, K.S., Chernyshov, D.O., & Dogiel, V.A., 2006, *ApJ*, 645, 1138
- [6] Clayton, D.D., 1973, *Nature Phys. Sci.*, 244, 137
- [7] Clayton, D.D., & Hoyle, F., 1974, *ApJ*, 187, 101
- [8] Dwek, E., et al., 1995, *ApJ*, 445, 716
- [9] Freudenreich, H.T., 1998, *ApJ*, 492, 495
- [10] Gillard, W., et al., 2006, these proceedings
- [11] Guessoum, N., Jean, P., & Gillard, W., 2005, *A&A*, 436, 171
- [12] Guessoum, N., Jean, P., & Prantzos, N., 2006, *A&A*, 457, 753
- [13] Jean, P., et al., 2003a, *A&A*, 407, L55
- [14] Jean, P., et al. 2003b, *A&A*, 411, L107
- [15] Jean, P., et al., 2006a, *A&A*, 445, 579
- [16] Jean, P., et al., 2006b, these proceedings
- [17] Johnson, W.N. III, Harnden, F.R. Jr., & Haymes, R.C., 1972, *ApJ*, 172L, 1
- [18] Kinzer, R.L., Purcell, W.R., & Kurfess, J.D., 1999, *ApJ*, 515, 215
- [19] Kinzer, R.L., et al., 2001, *ApJ*, 559, 282
- [20] Knödlseeder, J., et al., 2005, *A&A*, 441, 513
- [21] Knödlseeder, J., et al., 2006, these proceedings
- [22] Leventhal, M., MacCallum, C.J., & Stang, P.D., 1978, *ApJ*, 225, L11
- [23] Lingenfelter, R.E., & Hueter, G.J., 1984, in *High-Energy Transients in Astrophysics*, ed. S.E. Woosley, AIP, 558
- [24] Milne, P.A, et al., 2000, in *Proc. of 5<sup>th</sup> Compton Symposium*, AIP 510, 21
- [25] Milne, P.A, et al., 2001a, in *Proc. of the 4<sup>th</sup> INTEGRAL Workshop*, ESA SP-459, 145
- [26] Milne, P.A, et al., 2001b, in *Proc. of Gamma 2001*, AIP 587, 11
- [27] Milne, P.A, et al., 2002, *New Astron. Rev.*, 46, 553

- [28] Milne, P.A., 2006, *New Astron. Rev.*, 50, 548  
[29] Prantzos, N., Cassé, M., 1986, *ApJ*, 307, 324  
[30] Prantzos, N., 2004, in *Proc. of 5<sup>th</sup> INTEGRAL Workshop*, ESA SP-552, 15  
[31] Purcell, W.R., et al., 1997, *ApJ*, 491, 725  
[32] Ramaty, R., Stecker, F.W., Misra, D., 1970, *JGR*, 75, 1141  
[33] Ramaty, R., & Lingenfelter, R.E., 1979, *Nature*, 278, 127  
[34] Robin, A.C., et al., 2003, *A&A*, 409, 523  
[35] Rudaz, S., & Stecker, F.W., 1988, *ApJ*, 325, 16  
[36] Schanne, S., et al., 2006, these proceedings  
[37] Sizun, P., Cassé, M., & Schanne, S., 2006, *Phys. Rev. D*, 74, 063514  
[38] Strong, A.W., et al., *A&A*, 444, 495  
[39] Sturrock, P.A., 1971, *ApJ*, 164, 529  
[40] Teegarden, B, et al., 2004, in *Proc. of 5<sup>th</sup> INTEGRAL Workshop*, ESA SP-552, 819  
[41] Titarchuk, L., & Chardonnet, P., 2006, *ApJ*, 641, 293  
[42] Totani, T., 2006, *PASJ*, 58, 965  
[43] Vedrenne, G., et al. 2003, *A&A*, 411, L63, 2003  
[44] Wang, W., Pun, C.S.J., & Cheng, K.S., 2006, *A&A*, 446, 943  
[45] Weidenspointner, G., et al., 2003, *A&A*, 411, L113  
[46] Weidenspointner, G., et al., 2004, in *Proc. of 5<sup>th</sup> INTEGRAL Workshop*, ESA SP-552, 133  
[47] Weidenspointner, G., et al., 2006, *A&A*, 450, 1013

Model Component	Flux [ $\text{ph cm}^{-2} \text{s}^{-1}$ ]	$\lambda$
2 Nested Shells		1273.8
0–0.5 kpc Shell	$(3.88 \pm 0.34) \times 10^{-4}$	
0.5–1.5 kpc Shell	$(5.72 \pm 0.47) \times 10^{-4}$	
3 Nested Shells		1294.7
0–0.5 kpc Shell	$(3.88 \pm 0.34) \times 10^{-4}$	
0.5–1.5 kpc Shell	$(4.64 \pm 0.52) \times 10^{-4}$	
1.5–5 kpc Shell	$(8.05 \pm 1.76) \times 10^{-4}$	
4 Nested Shells		1302.1
0–0.5 kpc Shell	$(3.88 \pm 0.34) \times 10^{-4}$	
0.5–1.5 kpc Shell	$(4.92 \pm 0.53) \times 10^{-4}$	
1.5–5 kpc Shell	$(4.73 \pm 1.23) \times 10^{-4}$	
5–8 kpc Shell	$(13.6 \pm 5.04) \times 10^{-4}$	
2 Nested Shells and Young Disk		1310.7
0–0.5 kpc Shell	$(3.62 \pm 0.34) \times 10^{-4}$	
0.5–1.5 kpc Shell	$(4.74 \pm 0.49) \times 10^{-4}$	
Young Disk	$(1.11 \pm 0.18) \times 10^{-3}$	
3 Nested Shells and Young Disk		1318.2
0–0.5 kpc Shell	$(3.66 \pm 0.34) \times 10^{-4}$	
0.5–1.5 kpc Shell	$(4.21 \pm 0.53) \times 10^{-4}$	
1.5–5 kpc Shell	$(5.09 \pm 1.86) \times 10^{-4}$	
Young Disk	$(0.94 \pm 0.19) \times 10^{-3}$	
4 Nested Shells and Young Disk		1319.3
0–0.5 kpc Shell	$(3.68 \pm 0.34) \times 10^{-4}$	
0.5–1.5 kpc Shell	$(4.36 \pm 0.55) \times 10^{-4}$	
1.5–5 kpc Shell	$(4.86 \pm 1.87) \times 10^{-4}$	
5–8 kpc Shell	$(5.82 \pm 5.34) \times 10^{-4}$	
Young Disk	$(0.86 \pm 0.21) \times 10^{-3}$	
2 Nested Shells and Old Disk		1312.4
0–0.5 kpc Shell	$(3.72 \pm 0.34) \times 10^{-4}$	
0.5–1.5 kpc Shell	$(4.33 \pm 0.52) \times 10^{-4}$	
Old Disk	$(1.82 \pm 0.29) \times 10^{-4}$	
3 Nested Shells and Old Disk		1317.4
0–0.5 kpc Shell	$(3.76 \pm 0.34) \times 10^{-4}$	
0.5–1.5 kpc Shell	$(3.97 \pm 0.54) \times 10^{-4}$	
1.5–5 kpc Shell	$(4.33 \pm 1.93) \times 10^{-4}$	
Old Disk	$(1.52 \pm 0.32) \times 10^{-3}$	
4 Nested Shells and Old Disk		1318.0
0–0.5 kpc Shell	$(3.75 \pm 0.34) \times 10^{-4}$	
0.5–1.5 kpc Shell	$(4.11 \pm 0.57) \times 10^{-4}$	
1.5–5 kpc Shell	$(4.26 \pm 1.93) \times 10^{-4}$	
5–8 kpc Shell	$(4.35 \pm 5.55) \times 10^{-4}$	
Old Disk	$(1.41 \pm 0.35) \times 10^{-3}$	

*Table 1. The results of fits in which bulge and/or halo emission was modelled by nested shells of homogeneous emissivity, and disk emission was described by either the young or the old stellar disk model of Robin et al. [34].  $\lambda$  is the maximum likelihood ratio of the fits.*